



# Stochastic and deterministic dynamics in networks with excitable nodes



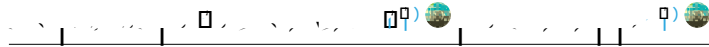
View Online



Export Citation



CrossMark



## AFFILIATIONS

<sup>1</sup>Department of Physics, Shahid Beheshti University, 1983969411 Tehran, Iran

<sup>2</sup>Department of Applied Mathematics, University of Colorado, Boulder, Colorado 80309, USA

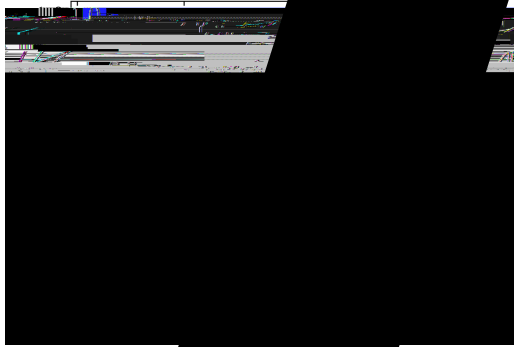
<sup>3</sup>Department of Physics, University of Mohaghegh Ardabili, 5619911367 Ardabil, Iran

<sup>a)</sup> **Authors to whom correspondence should be addressed:** [juanga@colorado.edu](mailto:juanga@colorado.edu) and [morteza.nattagh@gmail.com](mailto:morteza.nattagh@gmail.com)

## ABSTRACT

Networks of excitable systems provide a flexible and tractable model for various phenomena in biology, social sciences, and physics. A large class of such models undergo a continuous phase transition as the excitability of the nodes is increased. However, models of excitability that result in this continuous phase transition are based implicitly on the assumption that the probability that a node gets excited, its transfer function, is linear for small inputs. In this paper, we consider the effect of cooperative excitations, and more generally the case of a nonlinear transfer function, on the collective dynamics of networks of excitable systems. We find that the introduction of any amount of nonlinearity changes qualitatively the dynamical properties of the system, inducing a discontinuous phase transition and hysteresis. We develop a mean-field theory that allows us to understand the features of the dynamics with a one-dimensional map. We also study theoretically and numerically finite-size effects by examining the fate of initial conditions where



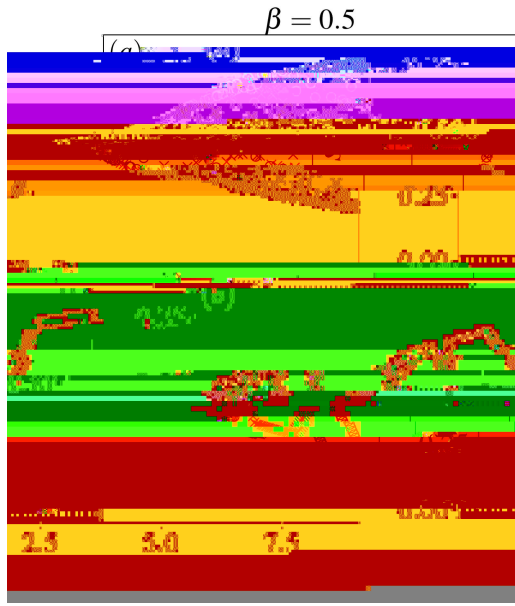


Transfer function ... between stochastic ... and deterministic

The dynamics generated by the Hopfield model presented in Sec. II, taking into account that nodes are in the refractory period, i.e., a node cannot spike immediately after being excited in the previous step, is given by a node  $i$  spikes at time  $t - 1$  is given by

$$h_i(t) = \sum_{j=1}^N A_{ij} x_j(t-1), \quad (5)$$

where  $x_j(t)$  is the state of node  $j$  at time  $t$  and zero otherwise, i.e., it is the effect of the previous spike. The transfer function  $h_i(t)$  is given by



Long-term values of even (circles) and odd (crosses) iterations of obtained from the mean-field map [Eq. (11)] as a function of  $\beta$  for  $\beta = 0.5$ . (a) The initial condition is random and uniformly chosen in  $[0, 1]$  for each  $s^0$ . (b) The initial condition is 0.01 for each  $s^0$ .

The sum over  $N$  in the previous equation can be interpreted as an average over nodes, which we will denote with  $\bar{s}^t$ . Assuming independence of the random variables  $A_{i,j}^t$  and  $h_{n-1}^t$ , we get

$$\mathbb{E}[\bar{s}^t] = \bar{s}^{t-1} h_{n-1}^t. \quad (9)$$

Now we use the fact that  $\bar{s}^t \approx \bar{s}^{t-1}$ . Furthermore, for an Erdős–Rényi network with large mean degree, the distribution of the random variable  $A_{i,j}^t$  is narrow about its mean,  $\bar{s}^t$ , so we can approximate  $h_{n-1}^t$  to obtain

$$\mathbb{E}[\bar{s}^t] = (1 - \beta)h(\bar{s}^{t-1}). \quad (10)$$

Focusing on the evolution of the expected value, we obtain the approximate one-dimensional map,

$$\bar{s}^t = f(\bar{s}^{t-1}) = (1 - \beta)h(\bar{s}^{t-1}). \quad (11)$$

Iteration of the map [Eq. (11)] with  $\bar{s}^0 = 0.1$  produces the black squares as shown in Fig. 2, which agree well with the simulations as  $N$  becomes large. Figure 3 shows the result of iterating the map [Eq. (11)] for  $\beta = 0.5$  with two different initial conditions for each value of  $\beta$ : for panel (a),  $\bar{s}^0$  is randomly and uniformly chosen in  $(0, 1)$ , and in panel (b),  $\bar{s}^0$  is always 0.01.

To demonstrate how the map Eq. (11) can shed light into the dynamics of the system, including its dependence on the initial conditions as shown in Fig. 3, we plot the second iterate of the map,  $f^{(2)}(s)$  vs  $s$  in Fig. 4 for  $\beta = 0.5$  and  $\beta = 1$  (top panel),  $\beta = 2$  (middle

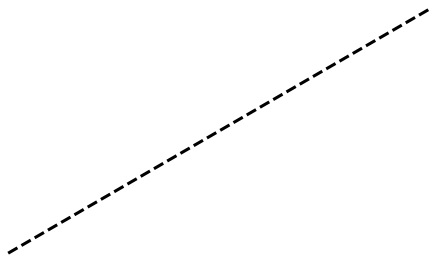
panel), and  $\beta = 5$  (bottom panel). For  $\beta = 1$ , the only fixed point is  $s = 0$ . As  $\beta$  increases, a stable positive fixed point is created at  $\beta = \beta_c$ , such that for  $\beta > \beta_c$ , there are two stable fixed points. For  $\beta = 5$ , there is a band of marginally stable period-2 orbits around  $s = 0.5$ . This band appears at  $\beta = 4$  and grows in size as  $\beta$  is increased. Note that even for this high value of  $\beta$ , the fixed point  $s = 0$  remains stable, as can be seen in the inset that shows the derivative  $f'(0)$  is less than one (it is, in fact, 0). The inset also shows that although the fixed point  $s = 0$  (the absorbing state) is stable, its basin of attraction is very small. With these observations, one can explain the qualitative features of Fig. 3 as follows. In panel (a) for  $\beta > 4$ , initial conditions that fall inside the band of fixed points alternate between two values, producing the cloud of points that grows in size as the size of the band grows. For  $\beta_c < \beta < 4$ , almost all initial conditions fall within the basin of attraction of the positive stable fixed point, but a few get attracted to the still stable fixed point  $s = 0$ . For  $\beta < \beta_c$ , all initial conditions get attracted to the stable fixed point  $s = 0$ . In panel (b), the initial condition  $\bar{s}^0 = 0.01$  belongs to the basin of attraction of  $s = 0$  up to approximately  $\beta = 3.7$ . Beyond that, the orbit gets attracted to the stable fixed point first and to a period-2 orbit thereafter.

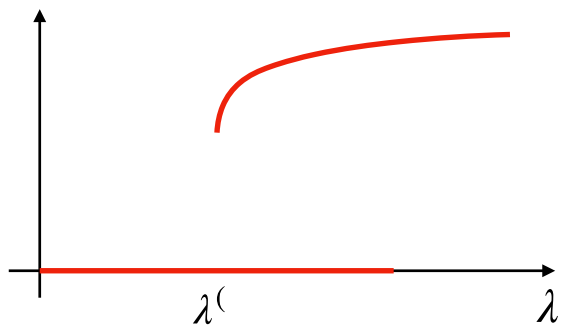
While some specific details about the bifurcation diagram depend on the shape of the transfer function  $h$  (such as the continuous band of marginally stable period-2 orbits), the general behavior of the system is as follows: for  $\beta = 0$ , there is a second-order phase transition from the subcritical to the supercritical regime, and a subsequent transition to an oscillatory regime. For  $\beta > 0$ , however, the transition is discontinuous and occurs at a value of  $\beta$  larger than one. The absorbing state  $s = 0$  remains stable, but its basin of attraction is extremely small. The phase diagram of the model is presented in Fig. 5.

## V. HYSTERESIS AND FINITE SIZE EFFECTS

In Sec. IV, we found that for  $\beta > 0$  the transition from the subcritical to the supercritical state is discontinuous. However, a mean-field analysis that assumed  $N \rightarrow \infty$  revealed that the absorbing state  $s = 0$  remains stable even for  $\beta > \beta_c$ . Therefore, it is important to understand how finite-size effects can drive the system away from the absorbing state. In this section, we address this by studying numerically and analytically the behavior of the system with initial conditions where only one node is excited, i.e.,  $s^0 = 1/N$ . Note that in the thermodynamic limit, and using the mean field description derived above, this would yield  $\bar{s}^t = 0$  for  $t > 0$  due to the linear stability of the absorbing state.

First, we study numerically the long-term behavior of the system under these initial conditions. For a given realization of the dynamics out of the oscillatory regime, the system either falls into the absorbing state  $\bar{s}^t \approx 0$  or it reaches a steady state with  $\bar{s}^t \approx \bar{s}_2 > 0$ . In Fig. 6(a), we show the probability distribution function (PDF) of  $\bar{s}$  in terms of  $\beta$  obtained from  $10^6$  realizations.





and using independence, we find

$$E[s_1]$$



state and the supercritical state, but the basin of attraction of the absorbing state is typically very small. The phase diagram for the system is shown in Fig. 5 in the limit  $N \rightarrow \infty$ .

We also studied the behavior of the model for large but finite networks. As a representative case of initial conditions consisting of a small number of excited nodes, we studied in detail the case of a single initially excited node. Using probabilistic arguments, we

which admits the solution  $p_i^t = e^{\lambda t} v_i$ , where  $v_i$  and  $\lambda$  are the eigenvector and (largest) eigenvalue of the  $A$  matrix. Equation (A1) holds for the case where at least one node can excite another node. Now let us consider the case where  $t \rightarrow 0$  excited nodes are necessary for exciting one node. Then this equation changes to

$$p_i^t = e^{\lambda t} v_i \left( 1 - p_i^t \right) \left[ 1 - \sum_{j=1}^N (1 - p_j^t A_{ij} A_i) \right], \quad (\text{A3})$$

which for small  $p$  limit and